DOI: 10.1002/ejoc.201500685

Water-Soluble Maleimide-Modified Gold Nanoparticles (AuNPs) as a Platform for Cycloaddition Reactions

Sara Ghiassian,[a] Pierangelo Gobbo,[a] and Mark S. Workentin*[a]

Keywords: Nanoparticles / Gold / Cycloaddition / Water chemistry

Maleimide-terminated triethylene glycol thiolate monolayer-protected gold nanoparticles (Mal-EG_4-AuNPs) with a core size of 2.5 ± 0.7 nm were prepared. Mal-EG_4-AuNPs were modified in high yields via interfacial 1,3-dipolar cycloaddition and Diels–Alder reactions with a variety of nitrones and dienes, respectively. The resulting cycloadduct-modified AuNPs were characterized using ^{1}H NMR spectroscopy and were verified by comparison of the spectra to those of the products of the model reactions with the same nitrones and dienes. TEM analysis showed that the reaction conditions did not affect the shape or size of the gold core, suggesting that this is an efficient methodology to modify small water soluble AuNPs under ambient pressure and biological temperature with high yields and a reasonable reaction time.

Introduction

Maleimides are important building blocks in organic synthesis and materials science, frequently employed in Michael addition, 1,3-dipolar cycloaddition or Diels–Alder reactions. Maleimide thiol/amine Michael addition has been utilized in the synthesis of cross linked polymers[1] such as hydrogels,[2] thermoset resins,[3] and coatings.[4] Furthermore, owing to the high yield and excellent selectivity of maleimide with thiols under physiological conditions, such chemistry is frequently employed for the surface immobilization of biomolecules.[5] There have been reports of methods for immobilizing biologically active ligands onto self-assembled monolayers of alkanethiolates on gold (SAMs). Mrksich et al. reported that SAMs presenting a maleimide functional group can be conveniently used for the preparation of biochips upon reaction with thiol-modified biologically active ligands.[6] A maleimide group at the interface of a AuNP allows for the exploitation of this type of reactivity in the use of the nanoparticle in applications such as drug or substrate delivery or as an optical marker for diagnostics in biological systems.[7]

The 1,3-dipolar cycloaddition is a highly useful reaction in generating a variety of structurally different heterocycles that can be desirable in pharmaceutics.[8] Of particular importance for synthetic purposes are the 1,3-dipolar cycloaddition reactions of nitrones which can lead to a variety of products by further manipulations of the initially formed isoxazolidine.[9] Furthermore, there are reports of 1,3-dipolar cycloadditions for polymer modification,[10] generation of nano-structured semiconductors,[11] surface modification of ordered mesoporous carbons,[12] synthesis of fluorescent single-walled carbon nano-tubes, which is used for the diagnosis and controlled drug delivery in medical field[13] and synthesis of modified DNA and RNA as molecular diagnostic tools.[14]

Another cycloaddition reaction that can be achieved using a maleimide platform is the Diels–Alder reaction, which is without a doubt one of the most versatile carbon–carbon bond forming reactions. Such chemistry is very important in natural product synthesis, as this often involves polycyclic compounds with many chiral centers, and a Diels–Alder reaction is often the only feasible route to these types of structures.[15] Furthermore, synthesis of macromolecules with advanced architectures can be achieved through the Diels–Alder strategy.[16]

These are just a few of many applications that having a maleimide functional group present, can offer. In 2006, we reported the functionalization of AuNPs with thiols bearing maleimide moieties.[17] The reactivity of these organic solvent-soluble maleimide/dodecane thiol-AuNPs was subsequently examined towards the Michael addition reaction,[18] the 1,3-dipolar cycloaddition,[19] and the Diels–Alder cycloaddition.[20] Although this contribution was an important step forward for their use as a template for building new architectures, it was limited to the use of a narrow range of organic solvents for further modification of AuNPs, while requiring long reaction times. To improve the reaction kinetics high pressure reaction conditions (11000 atm) were employed. Taking advantage of the negative activation volumes for such reactions resulted in notably shrinking the reaction times from days/weeks to minutes.[18–20] However, the fact that one would require a specific type of apparatus to reach such high pressures, limits the use of this method. Also, when it comes to the use of

[a] Department of Chemistry and the Center for Materials and Biomaterials Research, The University of Western Ontario, London, Ontario, N6A 5B7, Canada
Publish.uwo.ca/~mworkent

Supporting information for this article is available on the WWW under http://dx.doi.org/10.1002/ejoc.201500685.

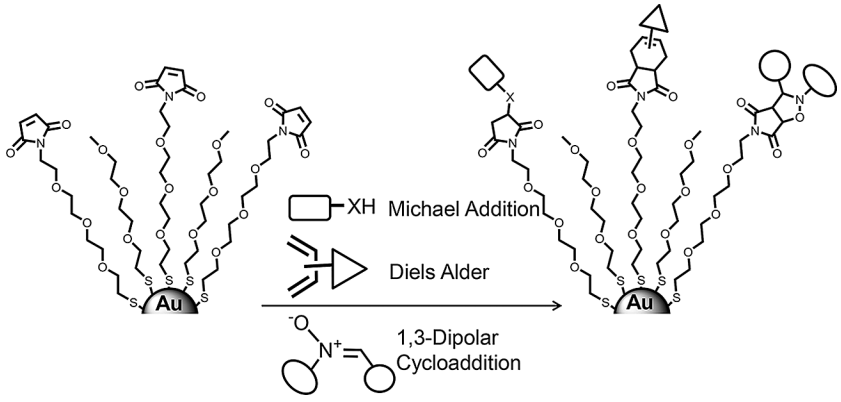

Scheme 1. Cartoon representation of Mal-EG_4-AuNPs and their versatile interfacial reactions: Michael addition, Diels–Alder, and 1,3-dipolar cycloaddition.

very delicate biological click partners, this method might not be as feasible.

Extending this methodology to water and polar solvent soluble AuNPs is advantageous as this will broaden the use of such AuNPs for applications where one is not limited to use of non-polar organic solvents only. However, use of maleimide in aqueous solutions is not without its challenges because the maleimide is prone to hydrolysis.[21]

Herein, we present a functionalization strategy via cycloaddition reactions to overcome these shortcomings using water soluble maleimide-functionalized AuNPs. Recently our group reported an efficient method to prepare small water-soluble maleimide-functionalized AuNPs utilizing a retro-Diels–Alder strategy based on the reversible cycloaddition reaction between furan and maleimide that avoids the hydrolysis of the maleimide as a complication.[21] The inherently broad substrate and solvent tolerance of this reaction makes it an ideal tool for the functionalization of nanomaterials and biomolecules.[22] In regards to maleimide functionalities, while Michael addition has been extensively studied, Diels–Alder and 1,3-dipolar cycloaddition reactions have remained rather unexplored. In the present publication, we report the modification of small water soluble maleimide-functionalized gold nanoparticle surfaces by use of the Diels–Alder and 1,3-dipolar cycloaddition reactions. The approach offers an excellent system to modify the surface of AuNPs with several different reactive partners, starting from a single-NP derivative that serves as a template for these types of reactions. This is a desirable strategy for introducing new functionalities to the AuNP surface while circumventing the need to synthesize new ligands from the ground up. Furthermore, the final AuNPs can be easily purified using dialysis or by washing the film of nanoparticles formed after solvent evaporation. Here we demonstrate the versatility of this approach using a small library of nitrones and dienes. We can take advantage of organic solvent solubility of these nanoparticles to avoid hydrolysis by carrying out all the interfacial reactions in polar organic media. The yields of all transformations are very high, and the reaction time is shorter than that of organic soluble maleimide/dodacane thiol-AuNPs previously reported.[19,20] All the AuNPs and cycloadducts remain soluble in water and a host of organic solvents. As illustrated in Scheme 1, the Michael partner, diene or nitrone can be incorporated into diverse range of substrates, expanding the scope of the utility of these maleimide-modified AuNPs. These groups, illustrated as geometric shapes in Scheme 1, can be small molecules, biomolecules, redox active species, or other nanomaterials to name a few. Hence one can take advantage of this versatile organic synthetic procedure utilizing maleimide gold nanoparticle template, to build a variety of novel architectures.

Results and Discussion

Our approach to prepare maleimide-functionalized AuNPs is shown in Figure 1. This methodology involves synthesis of methyl-terminated triethylene glycol monolayer-protected AuNPs (Me-EG_3-AuNPs). The methyl-terminated EG_3 ligands were selected as the base ligand on the nanoparticles because they impart both water and organic solvent solubility.[21] This is important because it enables us to prepare the maleimide-modified AuNPs (Mal-EG_4-AuNPs) under conditions that avoid water and the consequential undesired hydrolysis reaction of the maleimide moiety. This is very important when working with maleimide, as water can attack either of the two carbons of the imido group. Hence, maleimide functional groups gradually begin to hydrolyze into the non-reactive maleamic/maleic acid form.[21,23]

The required Me-EG_3-SH and furan-protected tetraethylene glycol maleimide thiol (FP-Maleimide-EG_4-SH) ligands were synthesized starting from the readily available triethylene glycol monomethyl ether (Me-EG_3-OH) and tetraethylene glycol (HO-EG_4-OH), respectively, following the previously reported procedures.[21] It is noteworthy that for the interfacial reactions occurring on the surface of AuNPs, the reactivity of the maleimide group can be impeded by the spectator ligands (i.e. triethylene glycol monomethyl ether) if the maleimide ligand has a shorter chain length than the spectator ligands. For this reason, the malei-

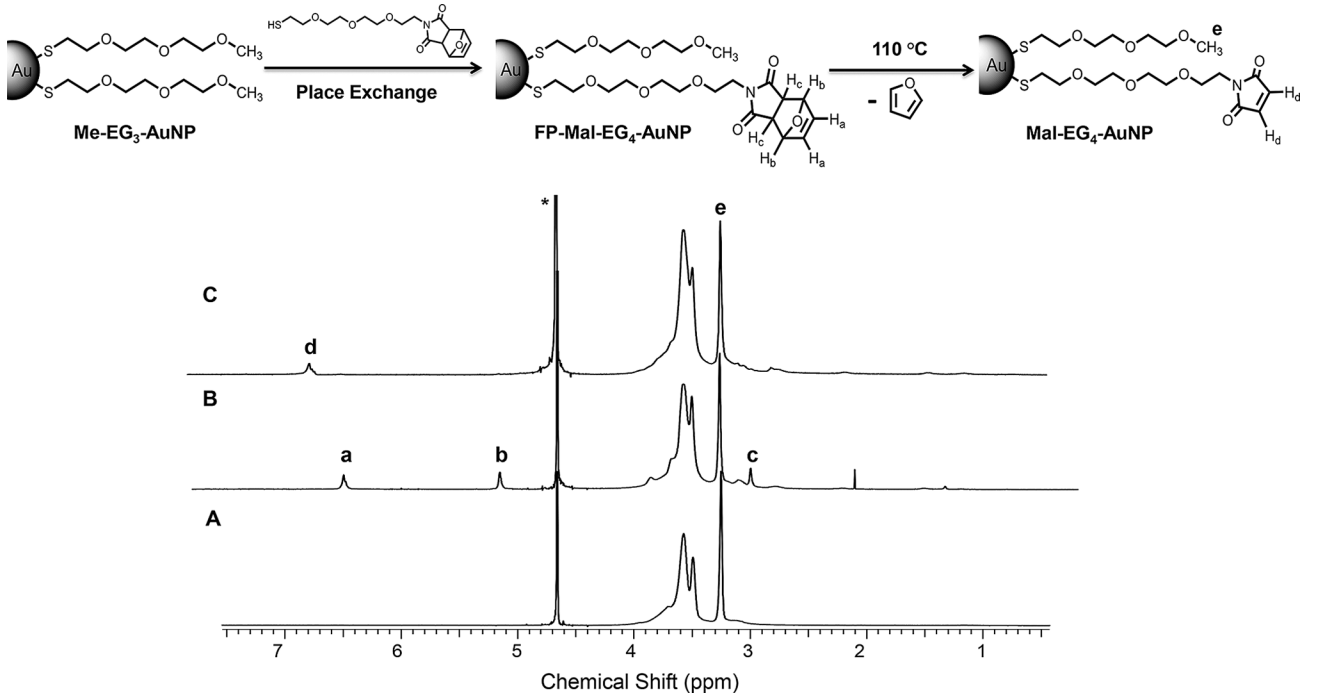

Figure 1. Schematic representation of the synthetic approach towards preparation of Mal-EG_4-AuNPs and the ^1H NMR spectra of: A) Me-EG_3-AuNPs, B) FP-Mal-EG_4-AuNPs, and C) Mal-EG_4-AuNPs; * signal of residual H_2O.

mide ligand was synthesized with one more ethylene glycol unit than the base ligand to lower the steric hindrance and make it more prone to reactivity. The Me-EG_3-AuNPs base nanoparticles were synthesized using a modified one-phase synthesis method according to previous reports.[21] To keep the nanoparticles in the 2–3 nm regime, a ratio of 1:3 (gold: thiol) was employed. The Me-EG_3-AuNPs were then subjected to place exchange reaction in the presence of the FP-Maleimide-EG_4-SH. Protection of the maleimide group is necessary in this step due to its reactivity towards the thiol groups present in the reaction mixture. This reaction was carried out in a mixture of methanol and acetone as solvent. After the place exchange, the solvent was evaporated to form a film of nanoparticles. This film was washed with cyclohexane (× 3) to remove the excess thiol **2**. The particles were then further purified by dialysis in water overnight. Finally, to prepare the desired template Mal-EG_4-AuNPs, deprotection of the maleimide at the AuNP interface was carried out through the retro-Diels–Alder reaction at 110 °C in toluene/acetonitrile (95:5) (Figure 1). Purification of the final AuNPs was straightforward: the solvent was evaporated to form a film of nanoparticles; this film was subsequently washed repeatedly using cyclohexane to remove the furan and any residual unbound thiol or disulfide that might be present.

The Mal-EG_4-AuNPs were characterized using transition electron microscopy (TEM), UV/Vis and NMR spectroscopy. The presence of the maleimide functionality on the AuNPs was initially confirmed by ^1H NMR spectroscopy. The ^1H NMR spectrum recorded in D_2O for the FP-Maleimide-EG_4-AuNP (Figure 1, **B**) exhibits the expected signals for the furan–maleimide adduct: (a) olefinic protons at δ = 6.60 ppm, (b) the protons adjacent to the bridged oxygen at δ = 5.25 ppm and (c) the two protons closer to the carbonyl groups at δ = 3.07 ppm. After the deprotection reaction and removal of the furan the signals corresponding to the Diels–Alder adduct at δ = 6.60, 5.25 and 3.07 ppm disappear along with the concurrent appearance of a signal at δ = 6.77 ppm that represents the alkene protons of the maleimide (d) (Figure 1, **C**). The ^1H NMR spectrum showed no indication of the double hydrolysis products that would have appeared as a signal at δ = 6.23 ppm due to the formation of maleic acid, or the mono hydrolysis product that would have shown two doublets at δ = 6.24 and 5.84 ppm due to the formation of maleamic acid.[21]

Through the integration of maleimide signal at δ = 6.77 ppm relative to the integration of the peak at δ = 3.38 ppm that corresponds to the three protons of the methyl group of the Me-EG_3-S ligands (e), it is possible to determine that approximately 30% of the protecting ligands are comprised of maleimide-terminated ligands, while 70% are methyl-terminated ones. This information allows for a more quantitative approach when following their interfacial reactivity in the subsequent steps.

TEM images reveal that the FP-Mal-EG_4-AuNPs are 2.2 ± 0.3 in size. According to these images there is no significant change in the size or shape of the gold core after the deprotection process as the average size of Mal-EG_4-AuNPs is 2.5 ± 0.7 nm. This confirms that the nanoparticles retained their structural integrity after being subjected to thermal deprotection. (images are displayed in the Supporting Information).

Subsequently the reactivity of Mal-EG_4-AuNPs towards the 1,3-dipolar cycloaddition and Diels–Alder reactions

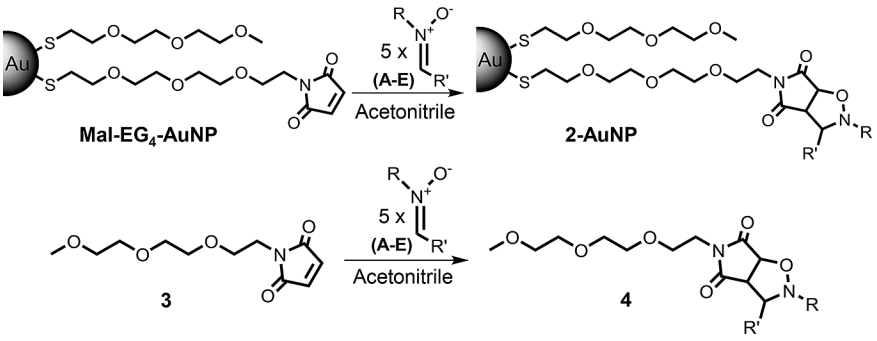

Scheme 2. 1,3-dipolar cycloaddition reaction of Mal-EG_4-AuNP and model compound 3 with nitrones **A**–**E** (see Table 1) to form the corresponding isoxazolidine-modified **2**-AuNPs and model isoxazolidine products **4**.

was investigated using a series of nitrones and dienes. In addition, because of the synthetic complexity of the cycloadducts formed using the Mal-EG_4-AuNP template, a model compound (methoxytriethylene glycol maleimide, compound **3**) was prepared that resembles the maleimide thiol incorporated on the surface of nanoparticles (see Scheme 2). In case of model reactions, we can easily follow the course of reaction using ^{1}H NMR spectroscopy observing the disappearance of the maleimide olefin protons signal at δ = 6.77 ppm and avoid NMR line broadening and loss of multiplicity caused by AuNPs which would hinder the characterization. All reactions were carried out under ambient pressure and biological temperature (1 atm, 37 °C).

The solvent can play a pivotal role in determining the reaction pathway, stereoselectivity and rate of reaction. Noteworthy is that, there have been reports of substantial to moderate rate enhancements for several Diels–Alder and dipolar cycloaddition reactions respectively when carried out in water.[24] However, knowing that maleimide can gradually hydrolyze in water,[21] we chose not to work in aqueous media to avoid more complicated NMR spectra due to the formation of hydrolysis products as well as the desired cycloadducts. To choose the best solvent for our experiments, we carried out two specific Diels–Alder and 1,3-dipolar cycloaddition reactions (1,3-dipolar cycloaddition between Mal-EG_4-AuNPs and nitrone **D** and Diels–Alder reaction of Mal-EG_4-AuNPs and diene **H**) using a variety of organic solvents while keeping all the other parameters constant. When following the reaction progress using ^{1}H NMR spectroscopy, more polar solvents such as methanol and acetonitrile proved to enhance the kinetics of both cycloaddition reactions to some extent compared to less polar solvents such as CH_2Cl_2 and $CHCl_3$. Based on this information along with lower solubility of our cycloaddition partners (nitrones and dienes) in highly polar protic solvents (such as water and methanol) we chose acetonitrile as the solvent media for all the subsequent cycloaddition reactions.

Nitrones are one of the most common species for 1,3-dipolar cycloaddition reactions owing to their ability to generate isoxazolidines with a high regio- and stereo-specificity. In the 1,3-dipolar cycloaddition reaction of nitrones with alkenes, up to three new contiguous chiral centers can be formed in the adduct. Furthermore, contrary to the majority of other 1,3-dipoles, most nitrones are stable compounds that do not require in situ formation.[25] To investigate the interfacial 1,3-dipolar cycloaddition of Mal-EG_4-AuNPs, a series of structurally diverse nitrones were synthesized (see Scheme 2 and Table 1) and their reactivity towards 1,3-dipolar cycloaddition with maleimide was evaluated by varying the stereoelectronic and steric character of substituents at both the C and N positions of the nitrone group. Since characterization of the cycloadducts is crucial to demonstrate the feasibility of our approach, incorporating features that can facilitate this step is advantageous. Having aryl groups present on the nitrones has the benefit of introducing aromatic protons into the final isoxazolidine structure, where the starting Mal-EG_4-AuNPs/model compound lack any signals. Hence these signals can be exploited in confirming the reaction progress. Furthermore, the inductive effect exerted by *N*-aryl-substituted nitrones was found to favor the reactivity by enhancing the dipolar nature of the nitrone (nitrone **A** or **D** compared to **B**). The presence of electron-donating substituents affects

Table 1. Time for completion of 1,3-dipolar cycloaddition reactions of Mal-EG_4-AuNPs and model compound **3** with nitrones **A**–**E** under ambient pressure and at 37 °C.

Nitrone	(4)	(2-AuNPs)
A	6 hours	20 hours
B	2 days	3 days
C	2 hours	5 hours
D	30 hours	2 days
E	4 days	6 days

the dipole character of the nitrones and decrease the reactivity (nitrone **B** compared to **E**). Steric hindrance was found to play a crucial role. Nitrones with less steric hindrance (such as nitrone **C**) work very efficiently in 1,3-dipolar cycloadditions. Because of the bulky character of the nanoparticles that imposes additional diffusional parameters and limits on the molecular orientation required for the reaction, sterically hindered nitrones were found to enhance the difference in the reaction kinetic between interfacial reaction and model reaction in solution (nitrone **A** and **D**). Finally, it is noteworthy that in case of furan-substituted nitrone **D** which contains both a diene and a nitrone groups available for cycloaddition, no Diels–Alder adduct of furan with maleimide was detected and it exclusively reacted through the 1,3-dipolar cycloaddition to form the corresponding isoxazolidine.

All of the interfacially prepared cycloadducts [**2**(**A**–**E**)-AuNPs] where compared to the corresponding model cycloadducts **4A**–**4E** using compound **3** as model maleimide molecule. Compound **3** was a useful model to study maleimide's cycloadditions, because it simplifies the analysis of the products by eliminating complications due to NMR line broadening and loss of multiplicity caused by the nanoparticles. In a typical reaction one equivalent of the Mal-EG_4-AuNPs/model maleimide compound **3** was dissolved in d_3-acetonitrile and five equivalents of the nitrone were added to it. Five times excess nitrone was used to ensure reaction completion, meanwhile not overwhelming the NMR spectrum to allow using the maleimide functionality signal to follow the reaction progress. Noteworthy is that, one can improve the reaction kinetics by introducing more excess amounts of the nitrone (>5×) to the system if using NMR to follow the reaction is not a concern. For each reaction, the time taken to completely convert the maleimide to the corresponding isoxazolidine was determined by recording ^{1}H NMR spectra at different time intervals. Reaction progress was monitored following the loss of the maleimide olefinic signal at δ = 6.77 ppm and the appearance of the new signals related to the cycloaddition product. Figure 2 illustrates the reaction progress of model compound **3** and nitrone **D**. As reaction proceeds the maleimide signal diminishes while new signals appear and start to grow corresponding to the isoxazolidine's protons. The results are summarized in Table 1. Both interfacial and the model reactions gave the cycloaddition product cleanly. As expected all nitrones react much more readily with the model maleimide molecule (ranging from hours to days) than towards the Mal-EG_4-AuNPs. In case of AuNPs, the mobility of functional thiols is limited, causing a pseudo-solid phase environment. Therefore the interfacial reactions taking place between interfacial functional groups on the nanoparticle and reactants can be substantially different from those taking place in a solution.

Full characterization, including NMR spectra for both model and interfacial reaction products for all the nitrones is provided in the supporting information. There are two diastereomers, the *endo* and the *exo* isomers, expected to form in these cycloadditions. In case of the model 1,3-dipolar cycloaddition reactions, these diastereomers were separated using preparative TLC and fully characterized by ^{1}H

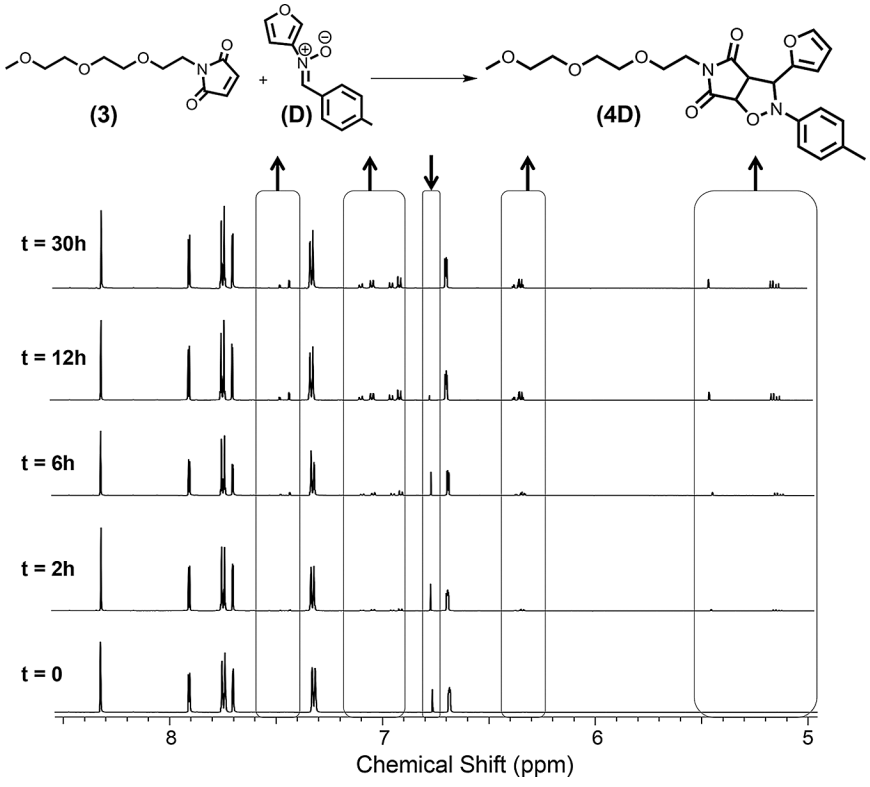

Figure 2. ^{1}H NMR spectra in 5–9 ppm region for the reaction of compound **3** and nitrone **D** at different time intervals.

and ^{13}C NMR spectroscopy and high resolution mass spectrometry. However, in case of interfacially produced isoxazolidines we are unable to separate the *endo* and *exo* products because they are formed as a mixture on a single AuNP. Figure 3 demonstrates a representative example comparing the products formed from the model reactions (**3** to **4**) to that on the AuNPs (Mal-EG_4-AuNP to **2**-AuNP) for nitrone **D**. After reaction completion and removal of the excess nitrone, ^1H NMR spectrum of the **2D**-AuNPs (Figure 3, **B**) matches entirely with those of the model **4D** (Figure 3, **C** and **D**). This confirms the modification of AuNPs with nitrone **D** and formation of the expected product.

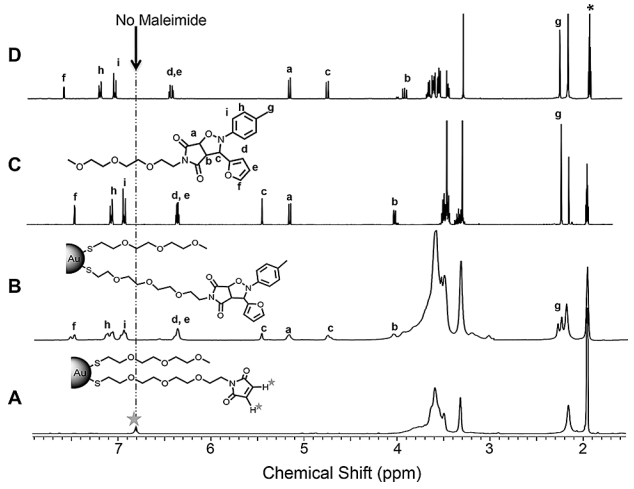

Figure 3. Representative ^1H NMR spectra of: A) Mal-EG_4-AuNPs and products from 1,3-dipolar cycloaddition reaction of Mal-EG_4-AuNPs with nitrone **D** to yield **B**) **2D**-AuNP as a mixture of diastreomers and compound **3** with nitrone **D** to yield **C**) **4D**-*exo* and D) **4D**-*endo* respectively. * signal of residual acetonitrile.

The reactivity of the Mal-EG_4-AuNPs towards the Diels–Alder reaction was also examined using a variety of dienes. As mentioned above, to facilitate the assignment of the protons of the ^1H NMR spectra, the reactions were also carried out using the solution-phase reaction of model compound **3** with the same dienes under the same reaction conditions as those used for AuNP modification to yield compounds **5F**–**5J** (Scheme 3). The results were then compared to those of the interfacially prepared cycloadducts, to confirm the formation of expected structures. To investigate the interfacial Diels–Alder reaction of Mal-EG_4-AuNPs, a series of dienes with different steric and electronic characters were employed (see Scheme 3 and Table 2). As expected, electron-rich and less sterically hindered dienes reacted much more readily with both the model compound and Mal-EG_4-AuNPs.

Table 2. Time for completion of 1,3-dipolar cycloaddition reactions of Mal-EG_4-AuNPs and model compound **3** with dienes **F**–**J** under ambient pressure and at 37 °C.

	Diene	(5)	(3-AuNPs)
F	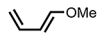	4 hours	20 hours
G		24 hours	3 days
H		10 hours	30 hours
I		3 days	7 days
J		30 hours	5 days

Similar to 1,3-dipolar cycloadditions, in a typical reaction one equivalent of the Mal-EG_4-AuNPs/model compound **3** was dissolved in d_3-acetonitrile and five equivalents of the diene were added to it. The progress of the reactions was monitored by ^1H NMR spectroscopy, following the appearance of signals from the cycloadducts and the disappearance of the maleimide olefinic proton signal. Figure 4 shows the ^1H NMR spectra for the Diels–Alder reaction of compound **3** with diene H at different time intervals. Absence of the signal at 6.77 ppm corresponding to the maleimide moiety was taken as completion of the reaction. The results for the Diels–Alder reactions of all the dienes are reported in Table 2. This information indicates that the reactions at the AuNP interface were always slower than in solution, reaching completion in the time scale of days instead of hours. This most likely is due to the bulky character of the AuNPs that imposes unique constraints on the orientation required for the reaction to occur causing a pseudo-solid-phase environment.

All the Diels–Alder reactions produced the expected *endo* isomer exclusively with the exception of diene **J** which yields a mixture of *endo* and *exo* isomers as demonstrated by NMR spectroscopy (see supporting information). Compounds **5F**–**5J** could be characterized more completely via

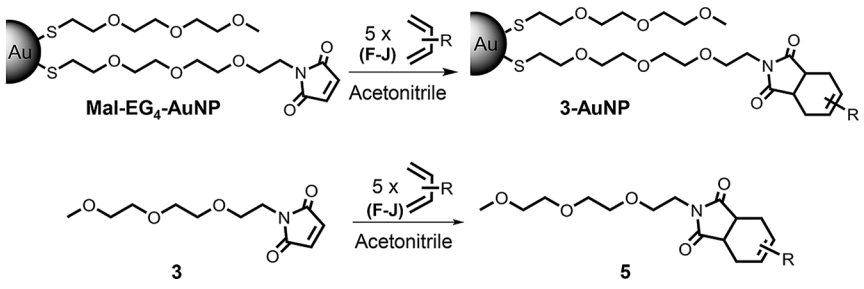

Scheme 3. Diels–Alder reaction of Mal-EG_4-AuNP and model compound 3 with dienes **F**–**J** (see Table 2) to form the corresponding modified **3**-AuNPs and model Diels–Alder cycloadducts **5**.

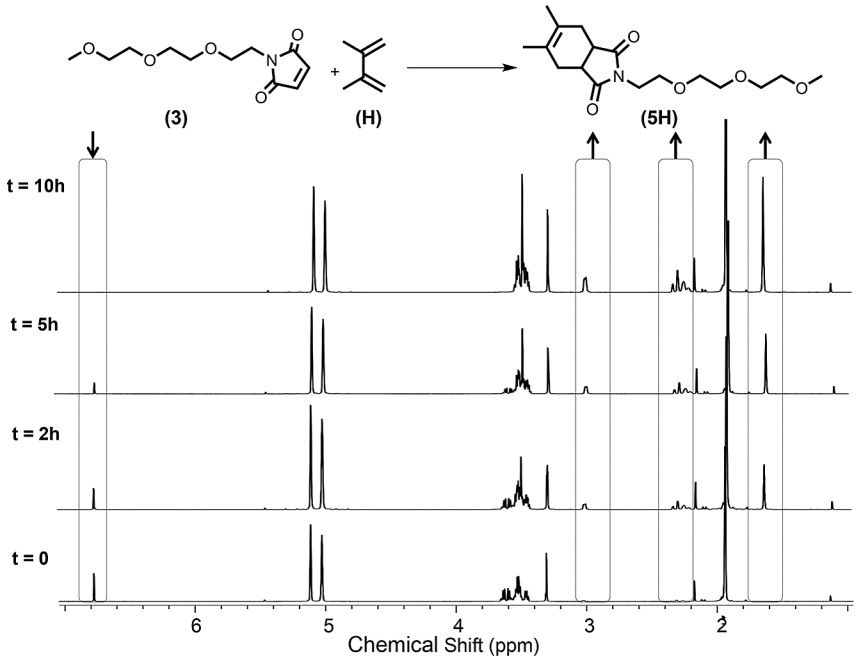

Figure 4. ^{1}H NMR spectra for the reaction of compound **3** and diene H at different time intervals.

^{1}H and ^{13}C NMR spectroscopy and high resolutuion mass spectrometry. ^{1}H NMR spectra of all the **3**-AuNP cycloadducts obtained are provided in the supporting information along with the spectral details of the corresponding reaction with the model compound **3**. Because the ^{1}H NMR spectra of **5F**–**5J** are not broad like those of **3**-AuNPs, they are more easily assignable, and hence they provide the confidence in the assignments of the spectra for **3**-AuNPs. For example, Figure 5 (**B** and **C**) exhibits the ^{1}H NMR spectra of **3H**-AuNPs and the model compound **5H**, respectively. The appearance of signals at δ = 1.62, 2.29 and 3.02 ppm and loss of maleimide signal at δ = 6.77 ppm in the ^{1}H NMR spectra of both **3H**-AuNP and **5H** indicate the essentially quantitative conversion of the maleimide-terminated ligand to the corresponding cycloadducts.

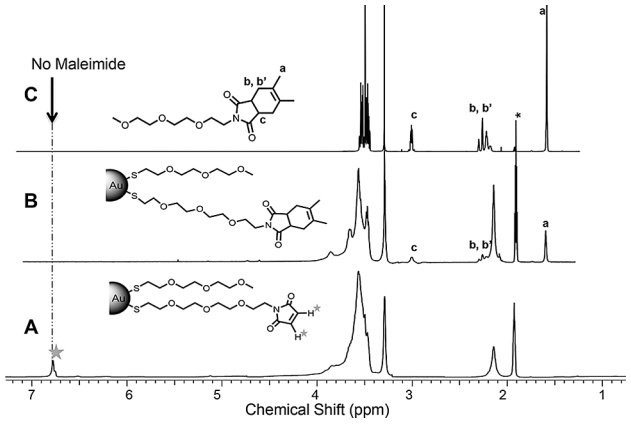

Figure 5. Representative ^{1}H NMR spectra of products from Diels–Alder reaction of: A) **1**-Mal-EG$_4$-AuNP with 2,3-dimethyl-1,3-butadiene to yield **B**) **3H**-AuNP and **3** with 2,3-dimethyl-1,3-butadiene to yield **C**) **5H**; * signal of residual acetonitrile.

To confirm that reaction condition does not affect the size and shape of the nanoparticles we used TEM. The average size of the Mal-EG$_4$-AuNPs was measured to be 2.5 ± 0.7 nm initially and 2.4 ± 0.9 nm after surface modification for the representative cycloadduct AuNPs (see Supporting Information). UV/Vis spectroscopy of all the AuNP cycloadducts was also carried out in water. None of the surface-modified AuNPs exhibit the plasmon band expected for larger AuNPs. This information along with the TEM images supports the fact that there is no distinct change in the size or shape of the gold core after the cycloaddition reactions.

Conclusions

In summary, we have developed a synthetic protocol for the facile addition of various functionalities to AuNPs bearing interfacial maleimide functionalities through cycloaddition reactions in high yields at ambient pressure and biological temperature (1 atm, 37 °C). The versatility of the method was demonstrated for the library of nitrones and dienes studied. This methodology has a variety of advantages over some other AuNP functionalization methods, including (i) more flexibility for the synthesis of desired AuNP conjugates, (ii) reduced reaction times compared to the previously reported organic solvent soluble AuNPs, and (iii) easy purification methods. Our results demonstrate the additional potential of the Mal-EG$_4$-AuNPs as a platform for cycloaddition reactions with any substrate bearing a diene or nitrone moeity. Due to the AuNPs' solubility in both water and a host of organic solvents, the application of these nanoparticles is not limited to a narrow range of solvents. Hydrolysis of the maleimide can be easily avoided

by carrying out all the interfacial reactions in organic solvents while maintaining the water solubility of the final cycloadduct AuNPs. The strategy we have introduced can be utilized for the development of novel nanomaterials and AuNP conjugates under mild reaction conditions, with potential applications in material chemistry, biology or nanomedicine.

Experimental Section

General Materials and Methods: The following reagents, unless otherwise stated, were used as received. Triethylene glycol monomethyl ether, tetraethylene glycol, 4-(dimethylamino)pyridine (DMAP), potassium thioacetate, deuterated acetonitrile (CD_3CN), deuterated chloroform ($CDCl_3$), tetrachloroauric acid trihydrate, sodium borohydride, *p*-toluenesulfonyl chloride, 1,3-pentadiene, 1-methoxy-1,3-butadiene, 2,3-dimethyl-1,3-butadiene, furfuryl alcohol, furan, and maleimide were purchased from Aldrich. All common solvents, triethylamine, magnesium sulfate, dry methanol, hydrochloric acid, sodium hydroxide, and potassium carbonate were purchased from Caledon. Deuterated water (D_2O) was purchased from Cambridge Isotope Laboratories. Ethanol was purchased from Commercial Alcohols. Glacial acetic acid (99.7%) was purchased from BDH. Maleic acid was purchased from Eastman Organic Chemicals. Dialysis membranes (MWCO 6000–8000) were purchased from Spectra/Por.

The ^1H and ^{13}C NMR spectra were recorded on either a Varian Inova 400 MHz or a Varian Mercury 400 MHz spectrometer. Transmission electron microscopy (TEM) images were recorded using a TEM Philips CM10. The TEM grids (Formvar carbon film on 400 mesh copper grids) were purchased from Electron Microscopy Sciences and prepared by drop casting solution of nanoparticles directly onto the grid surface. Mass spectrometry measurements were carried out using a Micro mass LCT (electrospray time-of-flight) mass spectrometer.

Synthetic Details

Compound 1 (OMe-EG$_3$-SH): All steps in the preparation of **1** were performed in accordance with the literature procedure.[21] Briefly, Me-EG$_3$-OH was tosylated to convert the hydroxyl group into tosyl. The tosylated Me-EG$_3$-OH was then converted into its corresponding thioacetate via an S_N2 reaction using potassium thioacetate. The thiol was obtained through basic hydrolysis of the thioacetate functionality. Compound **1** has been fully characterized earlier. To confirm the integrity of compound **1** we used ^1H and ^{13}C NMR spectroscopy that matches that of previous reports.[21] ^1H NMR (400 MHz, $CDCl_3$): δ_H = 1.60 (t, 1 H), 2.70 (q, 2 H), 3.41 (s, 3 H), 3.55 (m, 2 H), 3.63 (m, 8 H) ppm. ^{13}C NMR (400 MHz, $CDCl_3$): δ_C = 24.2, 59.0, 70.2, 70.5, 71.9, 72.9, 110.1 ppm.

Compound 2 (FP-Mal-EG$_4$-SH): All steps in the preparation of **2** were performed in accordance with the literature procedure.[21] HO-EG$_4$-OH was ditosylated, then one of the tosyl groups was treated with furan-protected maleimide and then the other tosyl extremity was converted into the thioacetate and subsequently hydrolyzed under basic conditions to generate the desired thiol, FP-Maleimide-EG$_4$-SH, as a light yellow oil. Compound **2** has been fully characterized before. To confirm the integrity of compound **2** we used ^1H NMR and ^{13}C NMR spectroscopy that matches that of previous reports.[21] ^1H NMR (400 MHz, $CDCl_3$): δ_H = 1.60 (t, 1 H), 2.70 (q, 2 H), 2.87 (s, 2 H), 3.65 (m, 14 H), 5.27 (s, 2 H), 6.52 (s, 2 H) ppm. ^{13}C NMR (400 MHz, $CDCl_3$): δ_C = 24.3, 47.5, 67.1, 70.1, 70.2, 70.5, 70.6, 72.6, 80.9, 136.5 ppm.

Compound 3 (1-{2-[2-(2-Methoxyethoxy)ethoxy]ethyl}-1*H*-pyrrole-2,5-dione): In a two-neck round-bottomed flask triethylene glycol monomethyl ether tosylate (1.45 g, 4.55 mmol) was dissolved in dry acetonitrile (100 mL). Then furan-protected maleimide (0.96 g, 6.75 mmol) was added to the mixture and it was stirred until everything dissolved. Next, K_2CO_3 (0.94 g, 6.80 mmol) was added and the reaction mixture was heated at 50 °C for 24 h. After reaction reached completion, the solvent was evaporated and the remaining oil was dissolved in dichloromethane and washed with water (× 3). The organic layer was then dried with $MgSO_4$. The crude product was purified using column chromatography (eluent: ethyl acetate) to give the furan-protected triethylene glycol monomethyl ether as a yellow oil. Next, the obtained product was dissolved in toluene and heated at 110 °C for 12 h to undergo the retro-Diels–Alder reaction. After evaporating the solvent, the crude product was purified using column chromatography (3:1 ethyl acetate/hexanes) to give the final product as light yellow oil. ^1H NMR (400 MHz, $CDCl_3$): δ_H = 3.36 (s, 3 H), 3.62 (m, 12 H), 6.70 (s, 2 H) ppm. ^{13}C NMR (400 MHz $CDCl_3$): δ_C = 37.1, 58.9, 67.7, 70.0, 70.5, 71.8, 134.1, 170.5 ppm. HRMS: calcd. *m/z* for $C_{11}H_{17}NO_5$ 243.1101, found 243.1107.

Furan-Protected AuNPs (FP-Mal-EG$_4$-AuNPs): Furan-protected maleimide-modified AuNPs were synthesized through a place exchange reaction. First, triethylene glycol monomethyl ether AuNPs (Me-EG$_3$-AuNPs) were synthesized in accordance with our previously reported procedure.[21] Next, to introduce the protected maleimide tetraethylene glycol thiol ligands onto the nanoparticle shell, freshly prepared thiol **2** (30 mg, 0.08 mmol) was dissolved in MeOH/acetone (4:1) (5 mL). This solution was then added to a solution of Me-EG$_3$-AuNPs [100 mg in 10 mL of MeOH/acetone (4:1)]. After vigorously stirring the reaction mixture for 15 min, the solvent was evaporated to form a film of nanoparticles. This film was washed with cyclohexane (× 3) to remove the excess thiol **2**. The particles were then further purified by dialysis in water overnight.

Maleimide-Functionalized AuNPs (Mal-EG$_4$-AuNPs): The deprotection of the maleimide was carried out using the retro-Diels–Alder reaction similar to that one reported previously for organic soluble maleimide AuNP. The FP-Mal-EG$_4$-AuNPs (500 mg) were dissolved in toluene/acetonitrile (95:5) (20 mL) in a round-bottomed flask equipped with a condenser. The system was then heated at 110 °C overnight. The solvent was evaporated under vacuum and the resulting nanoparticle film inside the flask was washed with cyclohexane (× 5).

Nitrones A–E: All the nitrones were prepared following the reference procedure. To a stirred solution of 5.0 g (1 equiv.) of the prerequisite aldehyde in 300 mL, 95% EtOH was added 2 equiv. of the nitro compound followed by 3.0 equiv. of powdered zinc. Finally, 6.0 equiv. of acetic acid was added dropwise at 0 °C and the mixture was allowed to stir at room temperature for 24 h. Following this time, the solvent was rotary-evaporated to half the original volume and the precipitated zinc was filtered off. The resulting liquid was purified by flash liquid chromatography elution (20–50% gradient of ethyl acetate to hexanes) to yield pure nitrone after rotary evaporation of the column fractions. All the nitrones have been characterized and reported previously.[26]

General Procedures for Cycloaddition Reactions of Maleimide

1,3-Dipolar Cycloaddition Reactions

Preparation of 2-AuNPs: Mal-EG$_4$-AuNPs (10 mg, 1 equiv.) was dissolved in deuterated acetonitrile (1 mL) and mixed with the ap-

propriate nitrone (5 equiv.) **A–E**. The mixture was then transferred to a NMR tube and placed in a 37 °C bath. After ^{1}H NMR spectroscopy showed reaction completion, the reaction was stopped by evaporating the solvent and forming a film of AuNPs. The products **2**(**A**–**E**)-AuNPs were then purified by washing the film with cyclohexane and then with 2-propanol to remove any unreacted nitrone. ^{1}H NMR spectroscopy was used to characterize the resulting **2**-AuNPs. These spectra were then compared to those of the products of the model reaction to ensure purity. All the NMR spectra are provided in the supporting information.

Preparation of 4A–4E: Compound **3** (20 mg, 1 equiv.) and nitrones **A**–**E** (5 equiv.) were dissolved in deuterated acetonitrile (2 mL). The mixture was then transferred to a NMR tube and placed in a 37 °C bath. After ^{1}H NMR spectroscopy showed reaction completion, the reaction was stopped and the product was purified by preparative TLC plate (20–50% gradient of hexanes to ethyl acetate). The resulting products were then characterized by ^{1}H and ^{13}C NMR spectroscopy and high resolution mass spectrometry. All the NMR spectra are provided in the supporting information.

Isoxazolidine 4A-*endo*: ^{1}H NMR (400 MHz, CD_3CN): δ = 3.27 (s, 3 H), 3.43 (dd, 2 H), 3.53–3.59 (m, 12 H), 3.77 (s,3 H), 3.9 (dd, 1 H), 4.67 (d, 1 H), 5.10 (d, 1 H), 6.87 (d, 2 H), 7.10 (m, 3 H), 7.25 (m, 4 H) ppm. ^{13}C NMR (400 MHz CD_3CN): δ_C = 39.6, 55.7, 56.3, 59.3, 67.8, 71.3, 71.4, 71.5, 72.6, 72.9, 78.2, 115.2, 121.9, 126.8, 127.9, 130.0, 130.7, 148.8, 161.1, 174.5, 176.5 ppm. HRMS: calcd. *m*/*z* for $C_{25}H_{30}N_2O_7$ 470.2043, found 470.2040.

Isoxazolidine 4A-*exo*: ^{1}H NMR (400 MHz, CD_3CN): δ_H = 3.24–3.32 (m, 5 H), 3.42–3.49 (m, 10 H), 3.75 (s,3 H), 3.87 (m, 1 H), 5.13 (d, 1 H), 5.36 (d, 1 H), 6.87 (d, 2 H), 6.90 (t, 1 H), 6.98 (d, 2 H), 7.18 (t, 2 H), 7.33 (d, 2 H) ppm. ^{13}C NMR (400 MHz CD_3CN): δ_C = 39.6, 56.3, 57.9, 59.3, 67.5, 70.4, 71.3, 71.4, 72.9, 78.2, 115.2, 116.7, 123.8, 130.2, 131.8, 149.3, 160.8, 175.6, 176.6 ppm. HRMS: calcd. *m*/*z* for $C_{25}H_{30}N_2O_7$ 470.2043, found 470.2038.

Isoxazolidine 4B-*endo*: ^{1}H NMR (400 MHz, CD_3CN): δ_H = 2.51 (s, 3 H), 3.28 (s, 3 H), 3.45 (m, 2 H), 3.53–3.58 (m, 10 H), 3.73 (t, 1 H), 3.81 (d, 1 H), 4.87 (d, 1 H), 7.24 (m, 2 H), 7.33 (m, 3 H) ppm. ^{13}C NMR (400 MHz CD_3CN): δ_C = 39.6, 43.4, 55.6, 59.3, 67.9, 71.3, 71.5, 73.0, 76.5, 78.0, 129.6, 129.7, 129.8, 135.9, 174.8, 177.0 ppm. HRMS: calcd. *m*/*z* for $C_{19}H_{26}N_2O_6$ 378.1782, found 378.1797.

Isoxazolidine 4B-*exo*: ^{1}H NMR (400 MHz, CD_3CN): δ_H = 2.41 (b, 3 H), 3.28 (s, 3 H), 3.45 (m, 2 H), 3.50–3.68 (m, 11 H), 3.75 (dd, 1 H), 4.96 (b, 1 H), 7.41 (m, 5 H) ppm. ^{13}C NMR (400 MHz $CDCl_3$): δ_C = 38.3, 58.9, 66.8, 70.0, 70.5, 71.9, 76.0, 128.3, 128.6, 128.8, 136.1, 175.1 ppm. two carbons could not be observed due to the weakness of the signals. HRMS: calcd. *m*/*z* for $C_{19}H_{26}N_2O_6$ 378.1782, found 378.1789.

Isoxazolidine 4C: ^{1}H NMR (400 MHz, CD_3CN): δ_H = 2.77 (b, 1 H), 3.28 (s, 3 H), 3.55–3.65 (m, 14 H), 3.76 (s, 3 H), 3.87 (s, 2 H), 4.76 (d, 1 H), 6.86 (d, 2 H), 7.2 (d, 2 H) ppm. ^{13}C NMR (400 MHz CD_3CN): δ_C = 39.5, 56.2, 59.2, 68.0, 71.33, 71.37, 71.4, 72.9, 114.9, 130.2, 131.3, 160.4, 177.9 ppm. HRMS: calcd. *m*/*z* for $C_{20}H_{28}N_2O_7$ 408.1887, found 408.1907.

Isoxazolidine 4D-*endo*: ^{1}H NMR (400 MHz, CD_3CN): δ_H = 2.25 (s, 3 H), 3.27 (s, 3 H), 3.43 (m, 2 H), 3.51–3.63 (m, 10 H), 3.88 (dd, 1 H), 4.70 (d, 1 H), 5.09 (d, 1 H), 6.33 (m, 2 H), 6.92 (d, 2 H), 7.08 (d, 2 H), 7.46 (dd, 1 H) ppm. ^{13}C NMR (400 MHz $CDCl_3$): δ_C = 38.1, 54.5, 55.1, 58.9, 66.6, 70.0, 70.50, 70.54, 71.1, 71.9, 76.5, 114.2, 119.4, 124.8, 126.1, 128.6, 128.7, 142.2, 159.7, 172.5, 174.6 ppm. HRMS: calcd. *m*/*z* for $C_{23}H_{28}N_2O_7$ 444.1887, found 444.1902.

Isoxazolidine 4D-*exo*: ^{1}H NMR (400 MHz, CD_3CN): δ_H = 2.21 (s, 3 H), 3.26 (m, 5 H), 3.42–3.48 (m, 10 H), 3.99 (dd, 1 H), 4.70 (d, 1 H), 5.11 (d, 1 H), 6.31 (m, 2 H), 6.88 (d, 2 H), 7.02 (d, 2 H), 7.41 (dd, 1 H) ppm. ^{13}C NMR (400 MHz $CDCl_3$): δ_C = 38.3, 53.6, 58.9, 63.9, 66.5, 70.1, 70.4, 70.5, 71.9, 76.2, 108.9, 110.5, 116.0, 125.3, 129.2, 132.8, 142.6, 150.0, 174.7 ppm. One of the carbonyl carbons was too weak to see. HRMS: calcd. *m*/*z* for $C_{23}H_{28}N_2O_7$ 444.1887, found 444.1898.

Isoxazolidine 4E-*endo*: ^{1}H NMR (400 MHz, CD_3CN): δ_H = 2.51 (s, 3 H), 3.28 (s, 3 H), 3.45 (m,2 H), 3.53–3.58 (m 10 H), 3.67 (t, 1 H), 3.75 (d, 1 H), 4.83 (d, 1 H), 5.95 (d, 2 H), 6.77 (m, 3 H) ppm. ^{13}C NMR (400 MHz $CDCl_3$): δ_H = 38.2, 42.4, 54.2, 59.0, 66.8, 69.9, 70.5, 71.9, 75.2, 76.2, 101.2, 107.8, 108.4, 121.6, 127.0, 147.9, 173.0, 175.6 ppm. HRMS: calcd. *m*/*z* for $C_{20}H_{26}N_2O_8$ 422.1680, found 422.1700.

Isoxazolidine 4E-*exo*: ^{1}H NMR (400 MHz, CD_3CN): δ_H = 2.37 (b, 3 H), 3.28 (s, 3 H), 3.44 (m, 2 H), 3.49–3.70 (m, 12 H), 4.91 (b, 1 H), 5.98 (s, 2 H), 6.84 (m, 3 H) ppm. ^{13}C NMR (400 MHz, $CDCl_3$): δ_C = 38.3, 42.3, 56.9, 59.0, 66.8, 70.0, 70.5 (×2), 71.9, 75.8, 101.3, 108.4, 122.2, 129.7, 147.8, 148.1, 175.1 ppm. One of the carbonyl carbons was too weak to see. HRMS: calcd. *m*/*z* for $C_{20}H_{26}N_2O_8$ 422.1680, found 422.1692.

Diels–Alder Reactions

Preparation of 3-AuNPs: Mal-EG_4-AuNPs (10 mg, 1 equiv.) was dissolved in deuterated acetonitrile (1 mL) and mixed the appropriate diene (5 equiv.) **F–J**. The mixture was then transferred to a NMR tube and placed in a 37 °C bath. After ^{1}H NMR spectroscopy showed reaction completion, the reaction was stopped by evaporating the solvent and forming a film of AuNPs. The products **3**(F–J)-AuNPs were then purified by washing the film with cyclohexane and then 2-propanol to remove any unreacted diene. ^{1}H NMR spectroscopy was used to characterize the resulting **3**-AuNPs. These spectra were then compared to those of the products of the model reaction to ensure purity. All the NMR spectra are provided in the supporting information.

Preparation of 5F–5J: Compound **3** (20 mg, 1 equiv.) and dienes **F**–**J** (5 equiv.) were dissolved in 2 mL of deuterated acetonitrile. The mixture was then transferred to a NMR tube and placed in a 37 °C bath. After ^{1}H NMR spectroscopy showed reaction completion, the reaction was stopped and the product was purified by preparative TLC plate (20–50% gradient of hexanes to ethyl acetate). The resulting products were then characterized by NMR spectroscopy. All the NMR spectra are provided in the supporting information.

Cycloadduct 5F: ^{1}H NMR (400 MHz, CD_3CN): δ_H = 2.4 (m, 2 H), 3.06 (m, 1 H), 3.12 (m, 1 H), 3.22 (s, 3 H), 3.28 (s, 3 H), 3.44 (m, 2 H), 3.48–3.57 (m, 10 H), 4.14 (m, 1 H), 6.06 (m, 2 H) ppm. ^{13}C NMR (400 MHz CD_3CN): δ_C = 23.5, 38.2, 39.1, 45.4, 57.1, 59.3, 68.1, 71.3, 71.4, 73.0, 73.4, 130.2, 132.0, 177.8, 181.3 ppm. HRMS: calcd. *m*/*z* for $C_{16}H_{25}NO_6$ 327.1674, found 327.1692.

Cycloadduct 5G: ^{1}H NMR (400 MHz, CD_3CN): δ_H = 1.28 (d, 3 H), 2.16 (m, 1 H), 2.45–2.55 (m, 2 H), 3.00 (dd, 1 H), 3.10 (dt, 1 H), 3.28 (s, 3 H), 3.43–3.53 (m, 12 H), 5.71 (m, 1 H), 5.81 (m, 1 H) ppm. ^{13}C NMR (400 MHz, CD_3CN): δ_C = 17.0, 24.3, 30.8, 38.6, 40.9, 44.8, 58.8, 67.7, 70.9 (×2), 72.5, 127.7, 135.5, 178.9, 180.7 ppm. HRMS: calcd. *m*/*z* for $C_{16}H_{25}NO_5$ 311.1725, found 311.1741.

Cycloadduct 5H: ^{1}H NMR (400 MHz, CD_3CN): δ_H = 1.64 (s, 6 H), 2.29 (m, 4 H), 3.02 (m, 2 H), 3.30 (s, 3 H), 3.45–3.55 (m, 12 H) ppm. ^{13}C NMR (400, MHz CD_3CN): δ_C = 19.9, 31.8, 39.3, 41.1, 59.3, 68.2, 71.2, 71.4, 73.0, 128.0, 181.5 ppm. HRMS: calcd. *m*/*z* for $C_{17}H_{27}NO_5$ 325.1881, found 325.1883.

Cycloadduct 5I: ^{1}H NMR (400 MHz, CD_3CN): δ_H = 2.85 (s, 2 H), 3.27 (s, 3 H), 3.42–3.57 (m, 12 H), 5.12 (dd, 2 H), 6.5 (d, 2 H) ppm. ^{13}C NMR (400 MHz, CD_3CN): δ_C = 39.3, 48.8, 59.3, 68.1, 71.3, 71.4 (×2), 73.0, 82.2, 137.8, 177.9 ppm. HRMS: calcd. *m*/*z* for $C_{15}H_{21}NO_6$ 311.1362, found 311.1343.

Cycloadduct 5J (inseparable mixture of *endo*/*exo*): ^{1}H NMR (400 MHz, CD_3CN): δ_H = 2.86/2.99 (d/d, 1 H), 3.12/3.20 (m/m/, 1 H), 3.28/3.29 (s/s, 3 H), 3.33/3.35 (s/s, 1 H), 3.41–3.58 (m, 12 H), 3.8–4.14 (m, 2 H), 5.11/5.20 (s/dd, 1 H), 6.28–6.41/6.5 (m/d, 2 H) ppm. ^{13}C NMR (400 MHz CD_3CN): δ_C, (*endo*/*exo*) signals indicated = 38.9/39.3, 46.9, 49.3/49.4, 59.2, 61.2/61.8, 68.0/68.1, 71.1, 71.3, 71.4, 72.9, 80.6/82.1, 83.1/93.7, 136.3/136.6, 138.1/139.3, 176.4/176.6, 177.7 ppm. HRMS: calcd. *m*/*z* for $C_{16}H_{23}NO_7$ 341.1467, found 341.1480.

Supporting Information: NMR spectra of compounds **3**, Me-EG_3-AuNP, FP-Mal-EG_4-AuNP, Mal-EG_4-AuNP, **2**-AuNPs, **3**-AuNPs and all the corresponding 1,3-dipolar cycloaddition and Diels–Alder cycloadducts from model reaction of **3** with dienes and nitrones. TEM images of FP-Mal-EG_4-AuNPs, Mal-EG_4-AuNPs, **2D**-AuNPs and **3H**-AuNPs, UV/Vis spectra of all the cycloadduct AuNPs are provided.

Acknowledgments

This work is supported by the Natural Sciences and Engineering Research Council of Canada (NSERC) under the Discovery Grants program and Western University Canada. P. G. thanks the Vanier CGS and Research Western for support.

[1] K. M. Mather, K. Viswanathan, K. M. Miller, T. E. Long, *Prog. Polym. Sci.* **2006**, *31*, 487–531.
[2] S. C. Rizzi, J. A. Hubbell, *Biomacromolecules* **2005**, *6*, 1226–1238.
[3] J. Pavlinec, N. Moszner, *J. Polym. Sci., Part A* **1997**, *10*, 165–178.
[4] B. Tamami, C. Betrabet, G. L. Wilkes, *Polym. Bull.* **1993**, *30*, 293–299.
[5] a) J. L. Zimmermann, T. Nicolaus, G. Neuert, K. Blank, *Nat. Protoc.* **2010**, *5*, 975–985; b) M. J. Roberts, M. D. Bentley, J. M. Harris, *Adv. Drug Delivery Rev.* **2002**, *54*, 459–476; c) R. T. Petty, H. W. Li, J. H. Maduram, R. Ismagilov, M. Mrksich, *J. Am. Chem. Soc.* **2007**, *129*, 8966–8967.
[6] B. T. Houseman, E. S. Gawalt, M. Mrksich, *Langmuir* **2003**, *19*, 1522–1531.
[7] a) S. Jain, D. G. Hirst, J. M. O'Sullivan, *Br. J. Radiol.* **2012**, *85*, 101–113; b) S. Manju, K. Sreenivasan, *J. Colloid Interface Sci.* **2012**, *368*, 144–151.
[8] a) P. Conti, C. Dallanoce, M. De Amici, C. De Micheli, K. N. Klotz, *Bioorg. Med. Chem.* **1998**, *6*, 401–408; b) W. C. Groutas, R. Venkataraman, L. S. Chong, J. E. Yoder, J. B. Epp, M. A. Stanga, E. H. Kim, *Bioorg. Med. Chem.* **1995**, *3*, 125–128.
[9] A. Padwa, W. H. Pearson, in: *Synthetic application of 1,3-dipolar cycloaddition chemistry toward heterocycles and natural products*, vol. 59, Wiley, New York, **2003**.
[10] a) I. Singh, Z. Zarafshani, J. F. Lutz, F. Heaney, *Macromolecules* **2009**, *42*, 5411–5413; b) Y. Lee, Y. Koyama, M. Yonekawa, T. Takata, *Macromolecules* **2009**, *42*, 7709–7717.
[11] S. Bakbak, P. J. Leech, B. E. Carson, S. Saxena, W. P. King, U. H. F. Bunz, *Macromolecules* **2006**, *39*, 6793–6795.
[12] X. Wang, D. E. Jiang, S. Dai, *Chem. Mater.* **2008**, *20*, 4800–4802.
[13] M. K. Bayazit, K. S. Coleman, *J. Am. Chem. Soc.* **2009**, *131*, 10670–10676.
[14] a) K. Gutsmiedl, C. T. Wirges, V. Ehmke, T. Carell, *Org. Lett.* **2009**, *11*, 2405–2408; b) F. Amblard, J. H. Cho, R. F. Schinazi, *Chem. Rev.* **2009**, *109*, 4207–4220; c) Z. M. Li, T. S. Seo, J. Y. Ju, *Tetrahedron Lett.* **2004**, *45*, 3143–3146.
[15] a) A. Gandini, D. Coelho, A. J. D. Silvestre, *Eur. Polym. J.* **2008**, *44*, 4029–4036; b) S. Y. Tang, J. Shi, Q. X. Guo, *Org. Biomol. Chem.* **2012**, *10*, 2673–2682.
[16] M. A. Tasdelen, *Polym. Chem.* **2011**, *2*, 2133–2145.
[17] J. Zhu, A. J. Kell, M. S. Workentin, *Org. Lett.* **2006**, *8*, 4993–4996.
[18] K. D. Hartlen, H. Ismaili, J. Zhu, M. S. Workentin, *Langmuir* **2012**, *28*, 864–871.
[19] J. Zhu, B. M. Lines, M. D. Ganton, M. A. Kerr, M. S. Workentin, *J. Org. Chem.* **2008**, *73*, 1099–1105.
[20] J. Zhu, M. D. Ganton, M. A. Kerr, M. S. Workentin, *J. Am. Chem. Soc.* **2007**, *129*, 4904–4905.
[21] P. Gobbo, M. S. Workentin, *Langmuir* **2012**, *28*, 12357–12363.
[22] a) P. Gobbo, M. C. Biesinger, M. S. Workentin, *Chem. Commun.* **2013**, *49*, 2831–2833; b) P. De, M. Li, S. R. Gondi, B. S. Sumerlin, *J. Am. Chem. Soc.* **2008**, *130*, 11288–11289.
[23] J. Kalia, R. T. Raines, *Bioorg. Med. Chem. Lett.* **2007**, *17*, 6286–6289.
[24] a) A. Meijer, S. Otto, J. B. F. N. Engberts, *J. Org. Chem.* **1998**, *63*, 8989–8994; b) R. Breslow, *Acc. Chem. Res.* **1991**, *24*, 159–164; c) M. R. Gholami, A. Habibi Yangjeh, *Int. J. Chem. Kinet.* **2000**, *32*, 431–434; d) P. S. Pandey, I. K. Pandey, *Tetrahedron Lett.* **1997**, *38*, 7237–7240.
[25] a) K. V. Gothelf, K. A. Jorgensen, *Chem. Rev.* **1998**, *98*, 863–909; b) K. B. G. Torssell, in: *Nitrile Oxides, Nitrones and Nitronates in Organic Synthesis*, VCH Verlagsgesellschaft, Weinheim, Germany, **1988**.
[26] M. D. Ganton, M. A. Kerr, *J. Org. Chem.* **2004**, *69*, 8554–8557.

Received: May 27, 2015
Published Online: July 20, 2015

